

# Study on Plasma Acceleration in Completely Electrodeless Electric Propulsion System<sup>\*)</sup>

Shuhei OTSUKA, Kohei Takizawa, Yuriko TANIDA,  
Daisuke KUWAHARA and Shunjiro SHINOHARA

Tokyo University of Agriculture and Technology, 2-24-16 Naka-Cho, Koganei, Tokyo 184-8588, Japan

(Received 25 November 2014 / Accepted 16 February 2015)

To solve a problem of a short lifetime due to a wear of the electrodes, we have been studying a completely electrodeless electric propulsion system. High-density ( $\sim 10^{13} \text{ cm}^{-3}$ ) helicon plasmas are being used for a dense source of our proposed system. Plasmas are accelerated by the Lorentz force in the axial direction, which is generated by the azimuthal current  $j_\theta$  induced in the plasma and the radial component of the external magnetic field  $B_r$ . Here, this  $j_\theta$  can be generated by a Rotating Magnetic Field (RMF) scheme proposed. As an initial try of the plasma acceleration, we have measured electron density  $n_e$  and ion velocity  $v_i$  using the RMF method, and found that  $n_e$  ( $v_i$ ) increased by a maximum of  $\sim 15\%$  ( $16\%$ ) compared to those without RMF. These results were the first step that shows experimentally the effectiveness of RMF acceleration scheme in the electrodeless electric propulsion system.

© 2015 The Japan Society of Plasma Science and Nuclear Fusion Research

Keywords: helicon plasma, electrodeless electric propulsion, rotating magnetic field, permanent magnet

DOI: 10.1585/pfr.10.3401026

## 1. Introduction

In recent years, a thruster which has a long lifetime and a high efficiency is required for the deep space exploration, for example, Jupiter or Neptune. An electric propulsion system is suitable for this exploration because its specific impulse (exhaust velocity divided by gravitational acceleration) is larger than chemical one, therefore this system has been studied extensively, leading to the practical operations. However, the lifetime of most current systems is short for use in deep space missions, because electrodes in the systems have direct contacts with plasmas, causing serious damages. In order to solve this problem, we have proposed completely electrodeless electric propulsion system called a Helicon Electrodeless Advanced Thruster (HEAT) [1–4]. In this system, both generation and acceleration methods of the dense plasma are executed by antennas from the outside of a discharge tube.

There are mainly two types of electromagnetic plasma acceleration methods in our team: acceleration [4, 5] by Rotating Magnetic Field (RMF) [6, 7] coils or a half cycle acceleration by an  $m = 0$  mode [5] coil. These act on a high-density ( $\sim 10^{13} \text{ cm}^{-3}$ ) helicon plasma [8–11], which is accelerated by the Lorentz force in an axial direction generated by the azimuthal current  $j_\theta$  induced in the plasma and the radial component of the magnetic field  $B_r$ . This field can be applied from the outside of permanent magnets and/or electromagnets, which have a divergent magnetic field [12]. In this paper, we will show initial experimen-

tal results on plasma acceleration using the RMF method, leading to the increase of ion velocity  $v_i$  as well as that of electron density  $n_e$  compared with no RMF case.

## 2. RMF Acceleration Scheme

The idea of RMF ( $j_\theta$  generation) [6, 7], which we proposed for acceleration of plasmas, comes from the Field Reversed Configuration (FRC) concept in a magnetically confined fusion field. Generation process of  $j_\theta$  based on the RMF method is shown in Fig. 1.

First, the rotating magnetic field  $B_\omega$  is generated by two pairs of RMF coils with AC currents which have a phase difference of 90 degrees between them, and then an axial electric field  $\tilde{E}_z$  is induced by Faraday's law. Second, an axial current  $\tilde{j}_z$  is generated by the effects of electron-ion collision and electron-neutral collision through Ohm's law,

$$\mathbf{E} - (\mathbf{j} \times \mathbf{B})/n_e e = \eta \mathbf{j}. \tag{1}$$

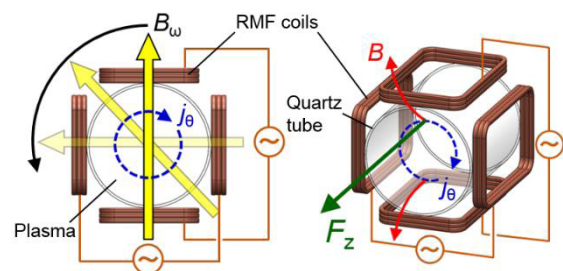


Fig. 1 Schematic of  $j_\theta$  generation for electrodeless plasma acceleration using RMF method.

author's e-mail: 50013643016@st.tuat.ac.jp

<sup>\*)</sup> This article is based on the presentation at the 24th International Toki Conference (ITC24).

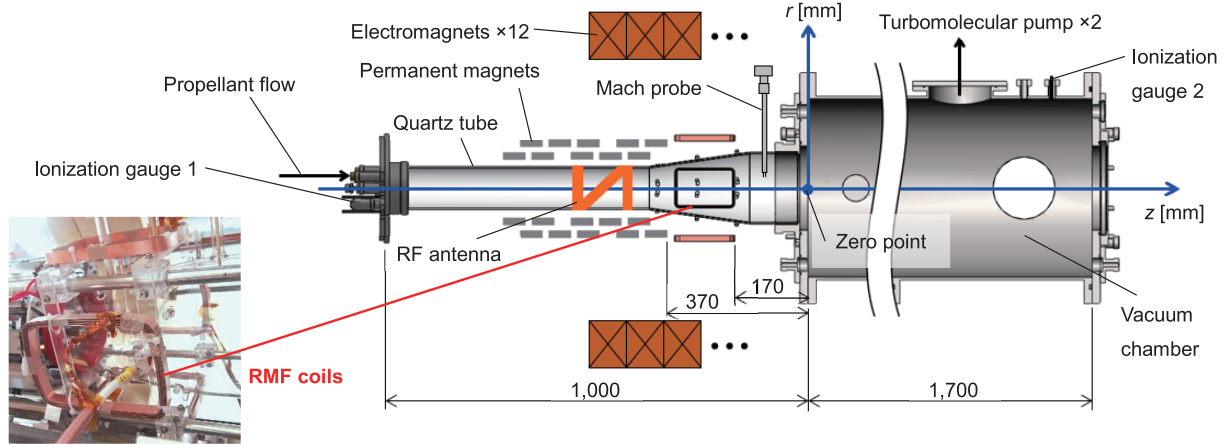


Fig. 2 Schematic of LMD with RMF scheme.

Third, electrons attain the steady azimuthal velocity  $v_{e\theta}$  by the balance of the steady accelerating torque generated by the nonlinear term of  $\tilde{j}_z \cdot \tilde{B}_r$  ( $\tilde{B}_r$  is radial component of  $B_\omega$ ) and the retarding torque generated by the collision effects again. In this way, azimuthal current  $j_\theta$  is produced as follows.

$$j_\theta = -n_e e v_{e\theta}. \quad (2)$$

Finally, the axial Lorentz force  $f_z$  for plasma acceleration is generated by this  $j_\theta$  and  $B_r$  applied from the external magnetic source,

$$j_\theta \times B_r = f_z. \quad (3)$$

Here,  $j_\theta$  is proportional to  $n_e$ , the strength of  $B_\omega$  and its rotation frequency  $f_{\text{RMF}}$  as long as the  $B_\omega$  penetration is satisfied ( $j_\theta$  is also proportional to RMF coil current  $I_{\text{RMF}}$  and the number of turns of coils before a saturation of rotation frequency of a electrons becoming an applied RMF frequency).

### 3. Experimental Device

#### 3.1 High-density helicon plasma source

Experiments were conducted in Large Mirror Device (LMD) [13] which can generate a high-density helicon plasma (Fig. 2). Specifications and typical operating conditions of LMD are shown in Table 1. A quartz tube (1,000 mm in axial length) has a tapered shape (100 ~ 170 mm in inner diameter) to prevent a wall loss of a divergent plasma, coming from the external magnetic field configuration. Here, we have permanent magnets and electromagnets, which are outside of the discharge tube.

#### 3.2 External magnetic field

Only permanent magnets were used as an external magnetic field in the present experiment. Figure 3 shows a magnetic field strength and its lines of permanent magnets in a divergent region [12]. Here, Neodymium magnet sheets ( $50 \times 25 \times 5 \text{ mm}^3$ ) of 300 were used, and their grade

Table 1 Specifications and typical operating conditions of LMD.

Axial length	1,700 mm
Inner diameter	445 mm
Background pressure	$\sim 10^{-4}$ Pa
Propellant	Ar gas
Discharge pressure	$\sim 0.1$ Pa
RF input power	$\sim 3$ kW
Excitation frequency	7 MHz

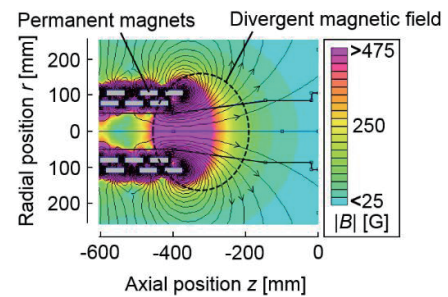


Fig. 3 Magnetic field strength and its field lines of permanent magnets in a divergent region.

was N35 made by NeoMag Co. Ltd.: 33 ~ 36 MGOe in maximum energy product and  $\sim 1,590$  G in surface magnetic flux density with the magnetization direction toward the center of a quartz tube. The maximum of  $B_r$  in the divergent region near the edge is  $\sim 150$  G, and RMF coils were placed in this region.

#### 3.3 RMF coils

Two pairs of RMF coils have 5 turns in each plane ( $168 \times 115 \text{ mm}$ ). Metal plates of coils bent is made of oxygen-free copper with 15 mm width and 0.5 mm thickness. The distance between facing coils is 225 mm, and an axial position of the coils is  $z = -170 \sim -320 \text{ mm}$  (see a tapered quartz region in Fig. 2) to take advantage of large  $B_r$  of permanent magnets for acceleration.

Table 2 Experimental conditions.

RF input power	1,000, 2,000, 3,000 W			
$f_{\text{RMF}}$	5 MHz			
Phase difference of $I_{\text{RMF}}$	90 degree in acceleration phase [ $\pm 90$ degrees, only in Exp. (1)]			
$I_{\text{RMF\_pp}}$	0 A	20 A	30 A	
$B_{\omega\_0p}$ (center)	0 G	$\sim 4$ G	$\sim 6$ G	
RMF total input power	0 W	$\sim 450$ W	$\sim 1,000$ W	
Gas flow rate	30 sccm	40 sccm	50 sccm	70 sccm
Gas pressure (Gauge 1)	0.54 Pa	0.83 Pa	0.90 Pa	1.17 Pa
Gas pressure (Gauge 2)	0.09 Pa	0.11 Pa	0.12 Pa	0.19 Pa

## 4. Results of RMF Acceleration

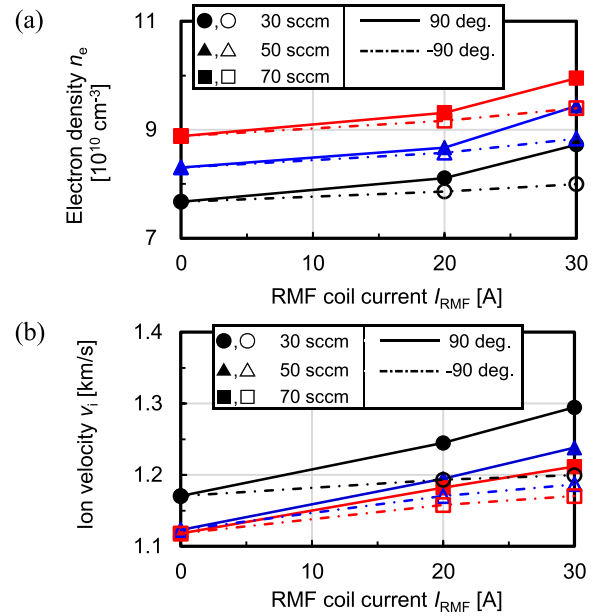
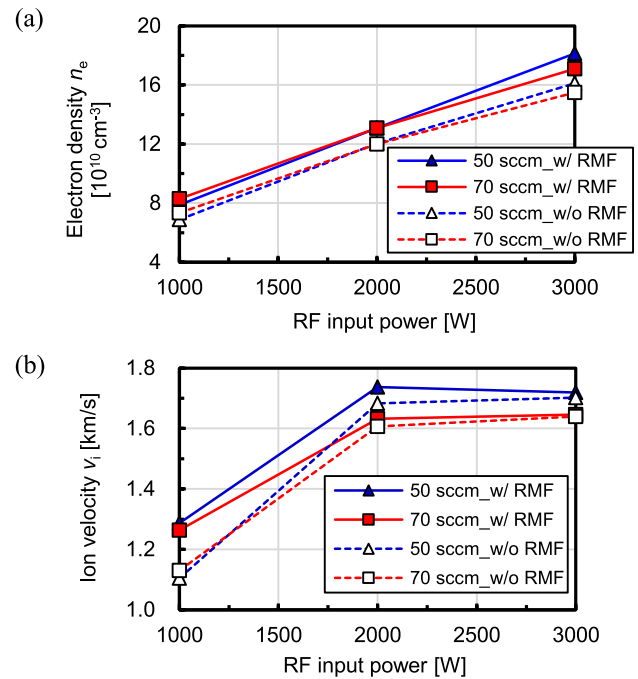
In order to verify the RMF acceleration effects, three types of experiments were carried out: (1)  $n_e$  and  $v_i$  in the axial direction by changing  $I_{\text{RMF}}$ . (2)  $n_e$  and  $v_i$ , in a fixed position, changing RF input power for the plasma generation, w/ and w/o RMF. (3) Radial distribution of  $n_e$  and  $v_i$ , w/ and w/o RMF. These experimental conditions including gas flow rate and its pressure are shown in Table 2 (measurement positions of gas pressure are shown in Fig. 2). Here, a Mach probe ( $z = -130$  mm) was used to measure  $n_e$  and  $v_i$ , employing the unmagnetized model (model constant  $\kappa = 1.26$ ) [14, 15].

### 4.1 Experiment (1)

Figure 4 (a) shows the dependence of  $n_e$  on  $I_{\text{RMF}}$ . In the case of acceleration phase ( $\varphi = 90$  deg.), increasing  $I_{\text{RMF}}$  from 0 A (w/o RMF) to 30 A,  $n_e$  was increased by  $\sim 14\%$  regardless of the gas flow rate. On the other hand, in the case of deceleration phase ( $\varphi = -90$  deg.), increasing  $I_{\text{RMF}}$ ,  $n_e$  was increased by  $\sim 5\%$  regardless of the gas flow rate. In Fig. 4 (b), in the case of  $\varphi = 90$  deg., increasing  $I_{\text{RMF}}$  from 0 A to 30 A,  $v_i$  was increased by  $\sim 11\%$ . However, in the case of  $\varphi = -90$  deg., increasing  $I_{\text{RMF}}$ ,  $v_i$  was increased by  $\sim 4\%$ . These results suggest a possibility that RMF has an effect to accelerate the plasma, but the phase difference study can be a future work.

### 4.2 Experiment (2)

Plasma behaviors using RMF depend on  $n_e$  and neutral density  $n_0$  through RF input power for the plasma generation, since this RMF method is governed by the particle collision effects (resistivity) and  $n_e$ , as shown in equations (2) and (3). From Fig. 5 (a), an increasing rate of  $n_e$  did not change appreciably regardless of the RF input power (this maximum rate was  $\sim 15\%$ ). On the other hand, this increasing rate of  $v_i$  in the case of low RF power of 1,000 W was greater than the higher RF power case, as shown in Fig. 5 (b). For example, in the case of 50 sccm gas flow rate, this increasing rate was  $\sim 16(1)\%$  in the case of 1,000 (3,000) W RF power. This suggests fading RMF acceleration effects when, e.g., an ionization degree increases, i.e., the electron-ion collision frequency increases.


 Fig. 4 (a)  $n_e$  and (b)  $v_i$ , changing  $I_{\text{RMF}}$  ( $r = 60$  mm and RF input power = 1,000 W).

 Fig. 5 (a)  $n_e$  and (b)  $v_i$ , changing RF input power for the plasma generation (in the case of  $I_{\text{RMF}} = 30$  A and  $r = 60$  mm).

### 4.3 Experiment (3)

In experiments (1) and (2), we measured  $n_e$  and  $v_i$  in the outer region of cylindrical plasma in order to observe RMF effects clearly. In experiment (3), radial profiles of  $n_e$  and  $v_i$ , w/ and w/o RMF methods were compared to see RMF acceleration effects. Figure 6 (a) shows that  $n_e$  increased in the almost whole radial region by RMF, and this increasing rate of  $n_e$  in the outer plasma region was slightly larger than the inner region by  $\sim 4\%$ . While  $v_i$  also increased in the almost whole region, w/ RMF, the increas-

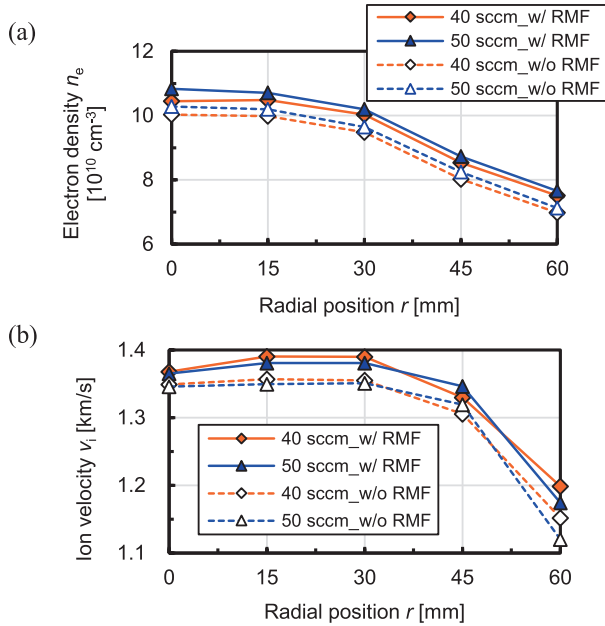


Fig. 6 Radial distributions of (a)  $n_e$  and (b)  $v_i$ , w/ and w/o RMF methods (in the case of  $I_{\text{RMF}} = 30$  A and RF input power = 1,000 W).

ing rate in  $r = 0 \sim 45$  mm region was almost constant with the larger rate found at  $r = 60$  mm, as shown in Fig. 6 (b).

There is a possibility that the penetration of  $B_\omega$  into plasmas might change the results. According to Milroy's expression for the magnetic field penetration [7], in our experimental conditions,  $B_\omega$  can penetrate partially into plasmas in  $r = 0 \sim 45$  mm region, but a preliminary measurement using a magnetic probe showed that  $B_\omega$  penetrated completely in all regions, leading to  $j_\theta$  generation conditions [see eq. (3)]. Therefore, if it is true, larger increasing rates of  $n_e$  and  $v_i$  than the present experiments could be obtained. It is necessary to measure  $j_\theta$  directly to clarify this, and also necessary to compare the penetration conditions experimentally with Milroy's expression, although it is difficult to estimate  $n_0$  experimentally.

## 5. Conclusion and Discussion

In this paper, we have shown the initial experimental results using the RMF acceleration method for a completely electrodeless electric propulsion system proposed, and it was confirmed that  $n_e$  and  $v_i$  increased mostly in the outer plasma region by this method. A preliminary measurement using a magnetic probe, a radial profile of radial component of magnetic field  $B_r$  (the magnitude with  $f_{\text{RMF}}$  frequency) did not show  $J_1$  (Bessel function) profile of azimuthal mode of  $m = 1$  expected from a helicon wave [9, 11]. Thus, the increases of  $n_e$  and  $v_i$  cannot be understood by the helicon wave alone, and  $j_\theta$  may be induced in the plasma. Since  $j_\theta$  can be estimated by radial profiles of  $B_z$  (the magnitude with  $2 f_{\text{RMF}}$  component, which is the same amplitude as the DC one of  $j_\theta$  from the nonlinearity [5]), the thrust increase by RMF (the Lorentz force)

is estimated to be  $\sim 20\%$ . This is consistent with the increasing rates of  $n_e$  and  $v_i$  obtained and also with the initial thrust measurements. Here,  $j_\theta$  generated by RMF effects becomes the largest when all electrons in the plasma have a complete rigid rotation to follow  $B_\omega$  of RMF. It is necessary to increase the value of  $B_\omega$  and to reduce the electron-neutral collision frequency (in other words, to reduce the neutral gas pressure) to satisfy the penetration condition. This means that it is necessary to increase the Hall parameter  $\gamma = \omega_{ce}/\nu$  in Milroy's expression ( $\omega_{ce}$ : electron cyclotron angular frequency, using the magnetic field of  $B_\omega$ ,  $\nu$ : the sum of electron-ion and electron-neutral collision frequencies).

Hereafter, we must survey the optimal experimental conditions ( $n_e$  of the target plasma,  $I_{\text{RMF}}$ ,  $B_\omega$ , etc.) in order to increase the efficiency by the RMF scheme. In addition, it is also important to introduce additional measurements such as the direct thrust by a developed pendulum-type thrust stand with a cylindrical target [16], plasma flows by spectroscopy or Laser Induced Fluorescence (LIF) methods [17] with reduced errors. Furthermore, we need to change a phase difference between two pairs of RMF currents in addition to 90 and  $-90$  degrees (acceleration and deceleration phases) to demonstrate clearly the acceleration effects: An initial check suggests a sinusoidal form of the increasing rates of  $n_e$  and  $v_i$  as a function of this phase, as we expected.

## Acknowledgments

We appreciate useful discussions made by the HEAT project members. This study has been partly supported by Grant-in-Aid for Scientific Research (S: 21226019) from the Japan Society for the Promotion of Science.

- [1] S. Shinohara *et al.*, Phys. Plasmas **16**, 057104 (2009).
- [2] S. Shinohara *et al.*, Proc. 32nd Int. Electric Propulsion Conf. IEPC-2011-056 (2011).
- [3] S. Shinohara *et al.*, Trans. Fusion Sci. Technol. **63**, 164 (2013).
- [4] S. Shinohara *et al.*, IEEE Trans. Plasma Sci. **42**, 1245 (2014).
- [5] T. Ishii *et al.*, JPS Conf. Proc. **1**, 015047 (2014).
- [6] I.R. Jones, Phys. Plasmas **6**, 1950 (1999).
- [7] R.D. Milroy, Phys. Plasmas **6**, 2771 (1999).
- [8] R.W. Boswell, Phys. Lett. **33A**, 457 (1970).
- [9] S. Shinohara, Jpn. J. Appl. Phys. **36**, 4695 (1997).
- [10] R.W. Boswell and F.F. Chen, IEEE Trans. Plasma Sci. **25**, 1229 (1997).
- [11] F.F. Chen and R.D. Boswell, IEEE Trans. Plasma Sci. **25**, 1245 (1997).
- [12] S. Otsuka *et al.*, Plasma Fusion Res. **9**, 3406047 (2014).
- [13] S. Shinohara *et al.*, Jpn. J. Appl. Phys. **35**, 4503 (1996).
- [14] M. Hudis and L. M. Lidsky, J. Appl. Phys. **41**, 5011 (1970).
- [15] K.S. Chung *et al.*, Phys. Fluids **B1**, 2229 (1989).
- [16] D. Kuwahara *et al.*, Plasma Fusion Res. **9**, 3406025 (2014).
- [17] N. Teshigahara *et al.*, Plasma Fusion Res. **9**, 3406055 (2014).